

International Conference on Space Optics—ICSO 2022

Dubrovnik, Croatia

3–7 October 2022

Edited by Kyriaki Minoglou, Nikos Karafolas, and Bruno Cugny,



Quantum Magnetometry for Space



Quantum Magnetometry for Space

C. Deans^{a,b}, T. Valenzuela^a, and M. G. Bason^a

^aRAL Space, UKRI-STFC Rutherford Appleton Laboratory, Didcot OX11 0QX, UK

^bNational Quantum Computing Centre, UKRI-STFC Rutherford Appleton Laboratory, Didcot OX11 0QX, UK

ABSTRACT

The ability to measure the magnetic fields around celestial bodies enables various insights into processes and phenomena deep within such bodies. The use of magnetometry in space missions dates back to the 1950s, and a number of different technologies have been used to measure these fields, ranging from fluxgates to Anisotropic Magneto Resistance (AMR) sensors. Optically-pumped magnetometers (OPMs) represent the state-of-the-art in magnetic field sensitivity.¹ Such sensors rely upon the interaction of laser light to spin polarise a warm vapour of neutral atoms. Detecting the precession of these spins, again with laser light, is a direct way to measure a magnetic field and is relatable to fundamental constants. Improvements in quantum technology within the last decade have led to the miniaturisation of these sensors. We have now reached the point where compact, lightweight, and low power devices offer greater sensitivity to magnetic fields than any other technology. In this work, we identify the following four key space application areas in which OPMs may offer significant advantages over existing technologies: Environments in which high sensitivity is needed at low magnetic fields (10s of nT), full vector read-out with high directional sensitivity and reduced SWaP compared to helium magnetometers, miniaturised and lightweight scalar magnetometers to complement vector fluxgate measurements, vector or scalar sensors that need high (40 dB) gradiometer performance.

This work identifies OPM configurations for each area and makes a first estimate of size, weight and power requirements for each. By enabling improvements in magnetic field sensitivity, this represents an exciting prospect for precision magnetic field measurements while also saving mass and reducing complexity.

Keywords: Magnetometry, Sensing, Quantum Sensing, Optically-pumped magnetometers

1. INTRODUCTION

The magnetic environment of the Earth and other bodies in the solar system varies by around five orders of magnitude, from tens of nanotesla in the outer heliosphere to hundreds of microtesla on Jupiter. As Table 1 indicates, it is important that the choice of magnetometer matches the expected magnetic field under study. A number of different technologies can typically meet such requirements. Thus, it is down to the size, weight and power (SWaP) and cost requirements that ultimately determines the most appropriate magnetometer for the mission.

2. TECHNOLOGY APPROACHES

This section provides an overview of multiple magnetometers. A summary of the relative performance of the various sensor types is given in Table 2.

2.1 Fluxgate magnetometers

The fluxgate magnetometer is the most common type of magnetic sensor used in space. It relies upon gating the ambient magnetic field by saturating a high permeability core.³ Through Lenz's law, an output coil picks up this changing flux, and an output voltage is produced. Gating a core at a frequency f , produces an AC voltage at $2f$. The signal amplitude provides information on the magnitude and direction of the ambient magnetic field. Many fluxgates have been successfully used in space thanks to their vector nature, low cost, and low power requirements.

E-mail: mark.bason@stfc.ac.uk

Table 1. Magnetic field strengths and accuracies.²

Environment	Range (nT)	Accuracy (nT)
Earth's field and LEO	0 - 45,000	0.1 - 1
Magnetospheres	0 - 10,000	0.05 - 0.2
Mercury	1,000	0.05 - 1
Venus	0 - 200	-
Moon	0 - 200	-
Mars	0 - 4,000	-
Jupiter	0 - 100,000	-
Saturn	0 - 20,000	-
Inner heliosphere	0 - 100	0.05 - 1
Outer heliosphere	0 - 30	0.01

Table 2. Typical specifications of a range of magnetometers.

Sensor technology	Sensitivity	Range (T)	Bandwidth	SWaP requirements	Vector/Scalar	Space Heritage
Fluxgate	$<5 \text{ pT}/\sqrt{\text{Hz}}$	$10^{-10} - 10^{-4}$	DC - kHz	Medium	Vector	Yes
Proton-precession	$150 \text{ pT}/\sqrt{\text{Hz}}$	$10^{-11} - 10^{-2}$	DC - 10s Hz	High	Scalar	Yes
AMR	$100 \text{ pT}/\sqrt{\text{Hz}}$	$10^{-10} - 10^{-4}$	DC - 100's Hz	High	Vector/Scalar	Yes
Helium	$<1 \text{ pT}/\sqrt{\text{Hz}}$	$10^{-8} - 10^{-4}$	DC - 100's Hz	Medium	Vector/Scalar	Yes
Alkali OPM	$10 \text{ fT}/\sqrt{\text{Hz}}$	$10^{-12} - 10^{-4}$	DC - 100's kHz	Medium	Vector/Scalar	Yes
NV Centres	$<1 \text{ nT}/\sqrt{\text{Hz}}$	$10^{-10} - 10^2$	DC - 10's MHz	Medium	Vector	No

2.2 Anisotropic Magneto-resistive (AMR) sensors

AMR sensors are based on elements whose resistance decreases when a magnetic field is applied.⁴ The sensor response is dependent on the direction of the magnetic field lines due to their anisotropic response. These sensors commonly use permalloy, which is magnetised in a certain direction, known as the easy direction. Upon application of a magnetic field, this magnetisation rotates towards the direction of the magnetic field with an angle-dependent on the external field strength. The changes in resistance are converted to a voltage using a two-legged current path which feeds two terminals on an operational amplifier. Operating in a closed-loop, fields of around 0.1 nT can be detected. These sensors are light, small, require between 0.1 and 0.5 mW of power, and can be operated at temperatures between -55°C and 200°C .

2.3 Proton precession/Overhauser magnetometers

The proton precession magnetometer is a scalar sensor that uses nuclear magnetic resonance to detect magnetic fields. The underlying principle is that many atoms possess a net magnetic moment and thus spin, or precess, in magnetic fields. The starting point of such a sensor is to align the atoms such that the magnetic moments point in the same direction, i.e. to polarise a sample. After such an alignment, the protons then relax in the ambient magnetic field. This relaxation takes the form of a change in the orientation of the magnetic moment, which rotates about the magnetic field. As it does so, an AC voltage is generated in a coil whose frequency is proportional to the magnitude of the field.⁵

The basic proton precession magnetometer uses a large volume, liquid sample rich in protons. The polarising fields are also high, 100 G or more. This, combined with the fact that the detectable ambient fields should be greater than 20 μT , has limited the utility of such sensors in space.

The Overhauser magnetometer improves on the proton precession magnetometer by polarising the sample more efficiently. A source of free radical electrons are added to the liquid sample and then pumped with radiofrequency radiation. Electron-proton coupling then acts to polarise the protons. This method is around ten times more efficient than the DC method and yields 100 times larger signals.⁶

2.4 Helium magnetometers

These magnetometers use a glass cell filled with He-4 – an inert, noble gas that is extremely stable. This gas is manipulated into a metastable state by an RF discharge. From this state, it is optically pumped using light at 1083 nm. Field-dependent magnetic resonances are then optically detected using an infrared photodetector. Scalar read-out can be achieved using magnetically-driven spin precession that causes transitions between three internal states of the atom.⁷ The magnetometer can also be configured as a vector sensor using either extra magnetic ‘bias’ fields to null the read-out or using modulation/demodulation techniques. Two types of optical pumping techniques are used for He magnetometers. Early versions used RF discharge lamps at 1083 nm, while later versions replaced this with pumping using semiconductor and fibre lasers. The latter, in particular, gives a high sensitivity below 1 pT/ $\sqrt{\text{Hz}}$.

Advantages of He-4 magnetometers include small heading errors and no ‘dead zones’ (angles at which the sensitivity of measuring the ambient magnetic field are drastically reduced). The drawback of such technology is in SWaP. A small He-4 magnetometer that uses less than 1 W of power is challenging because of the RF discharge and the lack of low-power (<10 mW) excitation lasers.

2.5 Optically-pumped magnetometers (OPMs) using alkali atoms

Optically-pumped magnetometers use light beams to redistribute atoms into magnetically sensitive states. Once in these states, atoms then precess around the ambient magnetic field. This precession is read-out by modulating another light field’s amplitude or plane of polarisation. Photodiodes are used to convert this probing light into an electrical signal. As the precession frequency, via the gyromagnetic ratio, is proportional to fundamental physical constants, these are absolute magnetometers. In contrast to proton precession magnetometers, OPMs exploit atoms (typically caesium, rubidium, or potassium) in the vapour phase. To increase the number of atoms that contribute to the magnetometer signal, the vapour is held in a glass cell and heated to 50 °C to 180 °C.

Many modern OPMs use miniature diode lasers, such as vertical-cavity surface-emitting lasers (VCSELs), to provide both the optical pumping and probing light. Such developments have significantly reduced the SWaP characteristics. The intended range of the magnetometer must be considered when designing the device. In sensors that use rubidium, the non-linear Zeeman effect presents problems with fields of over 10 μT . Schemes to overcome this difficulty using extra light beams have been demonstrated.⁸

2.6 Nitrogen-vacancy centres in diamond

Negatively-charged nitrogen-vacancy (NV) centres are point defects in a diamond lattice. The NV centre consists of a nitrogen atom adjacent to a carbon vacancy. The negatively-charged NV centre can be spin polarised using one wavelength of light, like in other optical magnetometers, and then read out at a different wavelength.⁹ The sensing element of NV centres are typically small and single defects can be engineered in nano-diamonds for high-resolution magnetometry.¹⁰ Researchers have been able to demonstrate field sensitivities of around nT/ $\sqrt{\text{Hz}}$. The sensor detects both DC and AC vector magnetic fields using different techniques - typically up to several GHz with bandwidths of up to roughly 100 kHz.

Table 3. Magnetometer instruments on a range of missions. A ‘✓’ indicates that the sensor was used on the spacecraft.

Mission	Launch Year	Destination	Fluxgate	Overhauser / Proton	Helium	Alkali OPM	AMR
Sputnik 3	1958	Earth	✓				
Mariner 4	1964	Mars			✓		
Kosmos 49	1964	-		✓			
POGO	1965 - 1969	Earth				✓	
Mariner 5	1967	Venus			✓		
Pioneer 10	1972	Jupiter			✓		
Pioneer 11	1973	Jupiter/Saturn	✓		✓		
ISEE-3	1978	Earth/Sun	✓		✓		
ISEE-3 (ICE)	1978	Comet	✓		✓		
Magsat	1979	Earth	✓			✓	
Ulysees	1990	Sun	✓	✓			
Cassini	1997	Saturn	✓		✓		
orsted	1999	Earth	✓	✓			
SAC-C	2000	Earth	✓		✓		
CHAMP	2000	Earth	✓	✓			
TRIO-CINEMA	2012	Earth					✓
SWARM	2013	Earth	✓		✓		
CSES	2018	Earth	✓			✓	
Solar Orbiter	2020	Sun	✓				
Radcube	2021	Earth					✓
NanoMagsat	-	Earth			✓		
JUICE	-	Jupiter & moons	✓			✓	

2.7 Historic magnetometer choices

In 3, we identify the magnetometer technologies used in space missions from the 1950s through to the present day. This table highlights the particularly wide-use of fluxgates, often in combination with Helium sensors. In addition, it indicates the range of technologies now available for space missions.

3. OPTICALLY-PUMPED MAGNETOMETERS

While the principles of optical pumping for magnetometry have been around for decades, having been the basis for lamp-pumped magnetometers in the 1960s, the advent of laser technology has greatly improved the sensitivity of OPMs while simultaneously reducing SWaP parameters. In addition, heading errors can be eliminated using dead-zone free configurations based on coherent population trapping (CPT).¹¹

3.1 OPM space heritage

Laser-pumped alkali atom magnetometers are beginning to attract the attention of the space community again. One example is the coupled dark-state magnetometer (CDSM). This is a scalar magnetometer, designed for the

China Seismo-Electromagnetic Satellite, which was launched in 2018. It was designed by Space Research Institute (IWF) of the Austrian Academy of Sciences. The CDSM uses CPT to reduce the sensitivity of the sensor to temperature. Unlike many other scalar OPMs, the detection scheme it uses is omnidirectional, i.e. has no dead zones. It is an all-optical sensor design without excitation coils or electromechanical parts. The instrument has a high accuracy of 0.19 nT, but a relatively large detection noise of $50 \text{ pT}/\sqrt{\text{Hz}}$ at 1 s integration time. It has a mass of 1.7 kg and power consumption of 3.4 W.¹²

Researchers at Johns Hopkins University and the National Institute of Standards and Technology (NIST) in the US have also developed a OPM for space applications.¹³ The focus of their work is not geared towards a particular space mission, rather in developing and qualifying the sensor. The collaboration used the rubidium isotope ^{87}Rb held in a vapour cell with a volume of only 1 mm^3 to enable efficient heating using a resistive heater implemented in multiple metal layers of a transparent sapphire substrate. The prototype instrument has a total mass of less than 0.5 kg and uses less than 1 W of power while achieving a sensitivity of $15 \text{ pT}/\sqrt{\text{Hz}}$ at 1 Hz, comparable to other OPMs. Their estimate of the combined variability due to solenoid field variations and instrument RMS noise amounted to about 0.1 nT. This is believed to be due to the power supply stability, which could easily be improved in future sensors.

3.2 All-optical sensors

In comparison to the electrical currents needed in many alternative sensing technologies, it is possible to produce OPMs that rely only upon the transmission and detection of light. One potential all-optical configuration is shown in Figure 1. In this approach the pumping and probing laser light is transferred to the cell and collected by optical fibres. Laser light, in combination with absorptive filters on the vapour cell faces, is also used to increase and stabilise the cell temperature.¹⁴

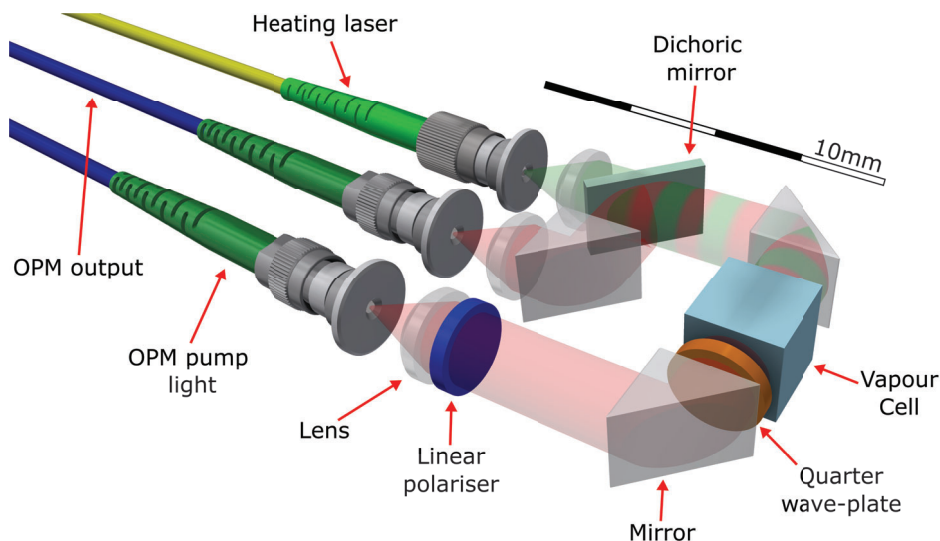


Figure 1. Example configuration of an all-optical OPM sensor for deployment in space.

An all-optical approach has two distinct advantages. The first is that the OPM can be passive, i.e. not produce magnetic fields itself, that would otherwise perturb other sensors. Secondly, the optical components that are used to guide light are significantly lighter than copper cabling. Reducing mass is particularly attractive to missions that place sensors at the end of a long boom. For example, a $125 \mu\text{m}$ diameter optical fibre used to connect a sensor at the end of a 3 m boom weighs around 400 g. A 32 AWG, $125 \mu\text{m}$ copper wire has a roughly $8.5 \times$ larger mass. Thus, moving to optical sensors could offer significant savings in boom design.

4. OPMS: KEY SPACE APPLICATION AREAS

4.1 Scalar OPMS to complement vector fluxgate measurements

Scalar magnetometers measure the Zeeman resonance frequency proportional to the absolute value of the magnetic field. They can operate in a range of fields, including in the Earth's magnetic field. These OPMS offer very high sensitivities of less than $1 \text{ fT}/\sqrt{\text{Hz}}$.¹⁵ Such performance is achieved by developing mitigations for detrimental atomic collisions, such as spin-exchange collisions, which are present in hot alkali-metal vapour magnetometers operating in a finite magnetic field. A collaboration between the Romalis group in Princeton and Twinleaf inc. demonstrated a finite field gradiometer using an intense pulsed laser to polarise a ^{87}Rb atomic ensemble and a compact VCSEL probe laser to detect paramagnetic Faraday rotation in a single multipass cell. They reported differential magnetic sensitivity of $14 \text{ fT}/\sqrt{\text{Hz}}$ over a broad dynamic range including Earth's field magnitude and common-mode rejection ratio higher than 10^4 .¹⁶

This application area is based on the fact that certain OPM schemes have the advantage of intrinsic calibration provided by fundamental physical constants. These constants govern the atomic vapour response to magnetic fields. As a result, they are able to provide exceptional accuracy and sensitivity with limited drift. The compact scalar sensors considered here are therefore well suited to act as an onboard calibration source for a more conventional vector fluxgate magnetometer. This hybrid sensor approach has been flown previously (as a fluxgate and helium magnetometer combination), for example on the Cassini mission, and has been shown to provide better accuracy than either instrument alone.

A simplified scalar magnetometer scheme has been developed with a specific focus on space applications. The prototype instrument achieved a sensitivity of $15 \text{ pT}/\sqrt{\text{Hz}}$ in a $10 \text{ }\mu\text{T}$ background field, with a total mass below 500 g and a power consumption below 1 W .¹³ The above approach uses an RF coil to drive the atomic response, typically in the M_x configuration.¹⁷ This has two potential drawbacks for space applications. The first is the addition of an electrical connection to the sensor to provide the RF coil drive. The second is that the M_x approach has two 'dead-zones', one perpendicular to (polar) and one parallel to (equatorial) the direction of propagation of the laser beam. If the measurement field approaches these regions, the measurement sensitivity drops. An alternative approach is to instead drive the atomic response by either frequency-modulation (Bell-Bloom magnetometer, or FM NMOR: frequency-modulated nonlinear magneto-optical rotation) or amplitude modulation (AM NMOR: amplitude-modulated nonlinear magneto-optical rotation) of the laser beam. A comparison of this approach with that of the M_x scheme has shown that the two have comparable sensitivities but that the NMOR scheme has the added simplicity of only requiring optical connections to the sensor unit and the removal of the equatorial dead-zone.¹⁸

Magnetometers based on this approach have been shown to achieve sub-picotesla sensitivities in Earth scale background fields ($10 \text{ }\mu\text{T}$). During operation, the modulation frequency tracks changes in the magnetic field. This tracking has been demonstrated across the 0 nT to $40\,000 \text{ nT}$ range. As a result, such schemes are ideal candidates for planetary missions – where large field ranges are encountered – in addition to being onboard calibration sources for alternative sensors.¹⁹ Finally, a simple extension to the sensor unit to include two non-overlapping orthogonal beams would allow continuous dead-zone-free measurements to be performed.

4.1.1 Scalar OPMS: Advantages

- Very accurate with high sensitivity, typically below $1 \text{ pT}/\sqrt{\text{Hz}}$
- Lightweight and few components
- Works in Earth-scale fields and can track magnetic field changes across a large range
- Can be modified to be made dead-zone free

4.1.2 Scalar OPMs: Space specification estimate

Following the analysis done in Korth, 2016,¹³ the power requirements are expected to be around 1 W with a total mass of 500 g. The OPM head is also compact - around $35 \times 25 \times 25 \text{ mm}^3$ and has a mass of around 50 g.

4.2 Vector read-out with low SWaP

Two vector components were measured by the Budker group in 2014.²⁰ Vector capability is achieved by effective modulation of the field along orthogonal axes and subsequent demodulation of the magnetic-resonance frequency. This modulation is provided by the AC Stark shift induced by circularly polarised laser beams. The sensor had a noise floor of $65 \text{ fT}/\sqrt{\text{Hz}}$ and $0.5 \text{ mrad}/\sqrt{\text{Hz}}$ and was limited by power and frequency noise in the laser beams. Extending this to a full vector magnetometer – i.e. measuring all three components of the magnetic field was achieved by the neutron electric dipole moment (nEDM) collaboration.²¹ This magnetometer uses four laser beams and is operated in a pulsed mode, with each experimental cycle repeating every 40 ms. The sensor was designed for long-time stability and achieves a scalar resolution better than 300 fT for integration times ranging from 80 ms to 1000 s. The magnetic field direction was measured with a resolution better than $10 \mu\text{rad}$ for integration times from 10 s up to 2000 s. In contrast to other vector magnetometers the scalar resolution is not degraded by extracting vector information.

In addition to these full vector techniques, scalar magnetometers can be adapted to yield 2D vector information by measuring both the DC probe light transmission and the AC signal at the Larmor frequency. Combining two sensors gives full vector read-out. While the angular sensitivity is better than 0.02° with a measurement time of 100 ms – systematic errors of around 1 degree currently prohibit greater uptake of this method.²² Vector information can also be extracted using OPM schemes with elliptically polarised light. However, these have relied upon the ability to change the direction of the bias field and dead zones were present.^{23,24} Typically, they would be of limited use in space missions.

Making use of the two naturally occurring isotopes of Rb, researchers have implemented all-optical vector magnetometers with two orthogonal optical pumping beams. Amplitude modulations occurred at ^{85}Rb and ^{87}Rb Larmor frequencies, respectively. Simultaneously detection of the magnetic field in each direction was extracted using a single probe beam in the third direction. In a magnetic field ranging from $10 \mu\text{T}$ to $50 \mu\text{T}$, a field angle sensitivity of better than $10 \mu\text{rad}/\sqrt{\text{Hz}}$ above 10 Hz was shown.²⁵

4.2.1 Vector OPMs: Advantages

- High sensitivity, around $10 \text{ fT}/\sqrt{\text{Hz}}$ to $100 \text{ fT}/\sqrt{\text{Hz}}$
- Full vector information. Angular sensitivity of $<1 \text{ mrad}/\sqrt{\text{Hz}}$ for long durations

4.2.2 Vector OPMs: Space specification estimate

The power requirements are expected to be around 2 W with a total mass of 1 kg. The OPM head could be relatively compact and would require just a vapour cell and mirrors. Thus, it could have a mass of tens of grams.

4.3 OPMs for low-field environments

A significant subset of OPMs are those designed to work at very low fields - *zero-field OPMs* typically operate in fields around 10 nT. At such fields, the rate of detrimental collisions of atoms in the vapour exceeds the rate at which they are precessing. This effectively averages out a large source of sample decoherence which would otherwise have detrimental effects on the sensitivity of the magnetometer. This regime is known as the Spin-Exchange Relaxation Free (SERF) regime. To operate in the SERF regime, the atomic density needs to be higher than in other classes of OPM. Increasing the temperature of the alkali vapour is the main method employed to reach this density.

World-record magnetic field sensitivities have been achieved in the zero-field/SERF regime: $0.54 \text{ fT}/\sqrt{\text{Hz}}$ with a measurement volume of 0.3 cm^3 . Despite this sensitivity, there is room for improvement, with a theoretical fundamental sensitivity limit of below $0.01 \text{ fT}/\sqrt{\text{Hz}}$.²⁶ Similar OPMs have also been operated as gradiometers. One such sensor from NIST has a baseline of 20 mm and is interrogated by the same laser beam resulting in a noise floor of $10 \text{ fT}/\sqrt{\text{Hz}}$ above 20 Hz. The maximum rejection of magnetic field noise is 1000 at 10 Hz.²⁷

While the operational range of zero-field OPMs is limited, there are a number of ways to extend this. Nulling coils can be used to compensate for external fields so that the field inside the OPM remains close to zero. This has been shown to work from 0 nT to 60 000 nT.²⁸ The range can also be extended by operating just outside the SERF regime, i.e. at lower vapour cell lower temperatures. This comes at the cost of reduced sensitivity via increased spin relaxation.

Full vector sensitivity has been demonstrated using a scheme in which an incident laser beam is reflected at 90° through a vapour cell and three orthogonal modulation fields are applied.²⁹ Such a magnetometer has magnetic-field sensitivities of $30 \text{ fT}/\sqrt{\text{Hz}}$ along two directions and $70 \text{ fT}/\sqrt{\text{Hz}}$ along the other axis.

An important consideration when using this OPM scheme is that, in comparison to other OPMs, they need careful calibration. In practice, this calibration can be done before the mission. Re-calibration is unlikely to be needed provided that there are not significant changes in sensor head temperature.

There are a range of environments in the solar system in which zero-field OPMs would be well suited (see Table 1). The magnetic fields of the moon are one such example. Miniature magnetospheres on the lunar surface are related to ‘lunar swirls’. These magnetospheres exhibit similar characteristics to normal planetary magnetospheres, namely, a collisionless shock. However, a crucial difference is that they are significantly smaller than those found on planets – on the order of several 100 km.³⁰ The Lunar Prospector recorded values in the tens of nanotesla.³¹ Interplanetary magnetic field measurements, such as the heliosphere, are also interesting candidates for measurement using zero-field OPMs. Some regions of space investigated by the current Solar Explorer mission are prime examples. Here, accuracies on the picotesla level are required - within the sensitivities of current OPMs.

Zero-field OPM development is a growth field, especially for studies of bio-magnetism. In this area, measurements of magnetic fields outside the body are used to provide information about the heart (magnetocardiography, MCG) and the brain (magnetoencephalography, MEG). As a result, one can expect future improvements both in SWaP and accuracy - driven by the commercial and scientific demands for improved sensors.

4.3.1 Low-field OPMs: Advantages

- Very high sensitivity, typically below $10 \text{ fT}/\sqrt{\text{Hz}}$
- Full vector information
- Lightweight and few components
- Minimal additional electronics needed

4.3.2 Low-field OPMs: Space specification estimate

The components of such a setup are not dissimilar from those in Korth, 2016.¹³ As such, the power requirements are expected to be around 1 W with a total mass of 500 g. The OPM head is also compact - around $35 \times 25 \times 25 \text{ mm}^3$ and has a mass of around 50 g.

4.4 Gradiometer measurements

Conventional space magnetometers are typically employed in a gradiometer configuration. Two or more sensors are used, often deployed on a boom extending from the spacecraft body. In the basic configuration, the sensor closer to the spacecraft monitors any electromagnetic interference (EMF) from the spacecraft. This signal can then be subtracted from the measurements of the second sensor to give a more accurate measure of the ambient magnetic field. Numerous approaches to gradiometer configuration and cancellation algorithms exist to maximise the gradiometer performance. Post-processing of the data combined with downlink rates often limits the time-frame for which the most accurate data is available to several days.

OPMs can be configured as gradiometers in the same multi-sensor approach as any other magnetic field sensor. This technique has been used to demonstrate applications including MEG, MCG, and low-field nuclear magnetic resonance (NMR). Miniature OPM gradiometers are currently close to commercialisation.³²

OPMs can also be configured as intrinsic gradiometers.^{33,34} When the probing laser beam passes back through the same cell (in a different location) – or through a second cell - the difference in the magnetic field between the two points is measured. This real-time subtraction removes the need for post-processing of the data, significantly increasing the speed at which it is available for investigation. The number of measurement components and electronics is also reduced in comparison to a multi-sensor setup.

4.4.1 Gradiometry: Advantages

- Intrinsic gradiometer measurements in real-time without post-processing
- All-optical approach
- Reduction in the number of measurement components
- Works in Earth scale fields
- Can be modified to track magnetic field changes across a large range

4.4.2 Space specification estimate

Power and weight requirements are approximately $2 \times$ that of the previous section: around 2W with a total mass of 750 g. The OPM head could be configured along a lightweight boom with each sensor being compact - around $35 \times 25 \times 25 \text{ mm}^3$ - and a mass of around 50 g.

5. CONCLUSION

OPMs represent the state-of-the-art in sensitive measurements of magnetic fields. Improvements in quantum technologies within the last decade have led to the miniaturisation of these sensors. We have now reached the point at which a compact and lightweight device offers more sensitivity to magnetic fields than any other technology. These developments open up multiple avenues of investigation - in particular for the measurement of magnetic fields in space.

In this work, we have identified four key areas in which OPMs may offer the largest advantages over existing techniques. For each, we made a first estimate of size, weight and power requirements. In addition, we looked at how all-optical sensors could enable significant mass reductions and avoiding copper cabling along long boom arms. Together with the improvements in magnetic field sensitivity, this represents an interesting prospect for precision magnetic field measurements in space.

ACKNOWLEDGMENTS

The authors wish to acknowledge the support of the UK Space Agency National Space Technology Programme (NSTP) Grants for Exploratory Ideas (GEI): “Quantum Magnetometry for Space GEI 1 – 03”. In addition, we thank M. Dunlop for stimulating discussions.

REFERENCES

- [1] Budker, D. and Jackson Kimball, D. F., [*Optical magnetometry*], Cambridge University Press (1 2011).
- [2] Olsen, N., Hulot, G., and Sabaka, T. J., “Measuring the earth’s magnetic field from space: Concepts of past, present and future missions,” in [*Space Science Reviews*], **155**, 65–93, Springer (8 2010).
- [3] Primdahl, F., “The fluxgate magnetometer,” *Journal of Physics E: Scientific Instruments* **12**(4), 241 (1979).
- [4] Jogschies, L., Klaas, D., Kruppe, R., Rittinger, J., Taptimthong, P., Wienecke, A., Rissing, L., and Wurz, M. C., “Recent developments of magnetoresistive sensors for industrial applications,” *Sensors* **15**(11), 28665–28689 (2015).
- [5] Cahill Jr, L. J. and Van Allen, J. A., “High altitude measurements of the earth’s magnetic field with a proton precession magnetometer,” *Journal of Geophysical Research* **61**(3), 547–558 (1956).
- [6] Hrvoic, I., “Overhauser magnetometers for measurement of the earth’s magnetic field,” in [*Proceedings of the Magnetic Field Workshop on Magnetic Observatory Instrumentation, Nurmijarvi, Finland*], 15–25 (1989).
- [7] Connor, B., “Space magnetics: The mariner v magnetometer experiment,” *IEEE Transactions on Magnetics* **4**(3), 391–397 (1968).
- [8] Schwindt, P. D., Lindseth, B., Knappe, S., Shah, V., Kitching, J., and Liew, L. A., “Chip-scale atomic magnetometer with improved sensitivity by use of the Mx technique,” *Applied Physics Letters* **90**, 081102 (2 2007).
- [9] Rondin, L., Tetienne, J.-P., Hingant, T., Roch, J.-F., Maletinsky, P., and Jacques, V., “Magnetometry with nitrogen-vacancy defects in diamond,” *Reports on progress in physics* **77**(5), 056503 (2014).
- [10] Taylor, J. M., Cappellaro, P., Childress, L., Jiang, L., Budker, D., Hemmer, P., Yacoby, A., Walsworth, R., and Lukin, M., “High-sensitivity diamond magnetometer with nanoscale resolution,” *Nature Physics* **4**(10), 810–816 (2008).
- [11] Ben-Kish, A. and Romalis, M. V., “Dead-zone-free atomic magnetometry with simultaneous excitation of orientation and alignment resonances,” *Physical Review Letters* **105**(19), 3–6 (2010).
- [12] Pollinger, A., Lammegger, R., Magnes, W., Hagen, C., Ellmeier, M., Jernej, I., Leichtfried, M., Kürbisch, C., Maierhofer, R., Wallner, R., Fremuth, G., Amtmann, C., Betzler, A., Delva, M., Prattes, G., and Baumjohann, W., “Coupled dark state magnetometer for the China Seismo-Electromagnetic Satellite,” *Measurement Science and Technology* **29**, 095103 (8 2018).
- [13] Korth, H., Strohhahn, K., Tejada, F., Andreou, A. G., Kitching, J., Knappe, S., Lehtonen, S. J., London, S. M., and Kafel, M., “Miniature atomic scalar magnetometer for space based on the rubidium isotope 87Rb ,” *Journal of Geophysical Research A: Space Physics* **121**(8), 7870–7880 (2016).
- [14] Wang, K., Zhou, B., Tang, J., Zhang, S., and Wang, Y., “Advances in laser heating of alkali vapor cells in magnetometers: a review,” in [*AOPC 2020: Optical Spectroscopy and Imaging; and Biomedical Optics*], Wang, Y., Sun, Y., Liu, J., Ling, Z., and Jin, D., eds., **11566**, 41, SPIE (11 2020).
- [15] Sheng, D., Li, S., Dural, N., and Romalis, M. V., “Subfemtotesla scalar atomic magnetometry using multi-pass cells,” *Physical Review Letters* **110**, 160802 (4 2013).
- [16] Lucivero, V. G., Lee, W., Romalis, M. V., Limes, M. E., Foley, E. L., and Kornack, T. W., “Femtotesla nearly quantum-noise-limited pulsed gradiometer at Earth-scale fields,” *Physical Review Applied* **18**, L021001 (8 2021).
- [17] Bell, W. E. and Bloom, A. L., “Optical detection of magnetic resonance in alkali metal vapor,” *Phys. Rev.* **107**, 1559–1565 (Sep 1957).
- [18] Jiménez-Martínez, R., Griffith, W. C., Wang, Y. J., Knappe, S., Kitching, J., Smith, K., and Prouty, M. D., “Sensitivity comparison of Mx and frequency-modulated bell-bloom Cs magnetometers in a microfabricated cell,” *IEEE Transactions on Instrumentation and Measurement* **59**, 372–378 (2 2010).
- [19] Pustelny, S., Wojciechowski, A., Gring, M., Kotyrba, M., Zachorowski, J., and Gawlik, W., “Magnetometry based on nonlinear magneto-optical rotation with amplitude-modulated light,” *Journal of Applied Physics* **103**, 063108 (3 2008).
- [20] Patton, B., Zhivun, E., Hovde, D. C., and Budker, D., “All-optical vector atomic magnetometer,” *Physical Review Letters* **113**, 013001 (7 2014).

- [21] Afach, S., Ban, G., Bison, G., Bodek, K., Chowdhuri, Z., Grujić, Z. D., Hayen, L., Hélaine, V., Kasprzak, M., Kirch, K., Knowles, P., Koch, H.-C., Komposch, S., Kozela, A., Krempel, J., Lauss, B., Lefort, T., Lemièrre, Y., Mtchedlishvili, A., Naviliat-Cuncic, O., Piegsa, F. M., Prashanth, P. N., Quémener, G., Rawlik, M., Ries, D., Rocchia, S., Rozpedzik, D., Schmidt-Wellenburg, P., Severjins, N., Weis, A., Wursten, E., Wyszynski, G., Zejma, J., and Zsigmond, G., “Highly stable atomic vector magnetometer based on free spin precession,” *Optics Express* **23**, 22108 (8 2015).
- [22] Zhang, R., Mhaskar, R., Smith, K., Balasubramaniam, E., and Prouty, M., “Vector measurements using all optical scalar atomic magnetometers,” *Journal of Applied Physics* **129**, 044502 (1 2021).
- [23] Su, S., Zhang, G., Bi, X., He, X., Zheng, W., and Lin, Q., “Elliptically polarized laser-pumped M x magnetometer towards applications at room temperature,” *Optics Express* **27**, 33027 (11 2019).
- [24] Zheng, W., Su, S., Zhang, G., Bi, X., and Lin, Q., “Vector magnetocardiography measurement with a compact elliptically polarized laser-pumped magnetometer,” *Biomedical Optics Express* **11**, 649 (2 2020).
- [25] Cai, B., Hao, C. P., Qiu, Z. R., Yu, Q. Q., Xiao, W., and Sheng, D., “Herriott-cavity-assisted all-optical atomic vector magnetometer,” *Physical Review A* **101**, 053436 (5 2020).
- [26] Kominis, I. K., Kornack, T. W., Allred, J. C., and Romalis, M. V., “A subfemtotesla multichannel atomic magnetometer,” *Nature* **422**, 596–599 (4 2003).
- [27] Sheng, D., Perry, A. R., Krzyzewski, S. P., Geller, S., Kitching, J., and Knappe, S., “A microfabricated optically-pumped magnetic gradiometer,” *Applied Physics Letters* **110**, 031106 (1 2017).
- [28] Li, J., Deng, Y., Wang, X., Lu, H., and Liu, Y., “Miniature Wide-range Three-axis Vector Atomic Magnetometer,” *IEEE Sensors Journal* **21** (2021).
- [29] Xiao, W., Wu, Y., Zhang, X., Feng, Y., Sun, C., Wu, T., Chen, J., Peng, X., and Guo, H., “Single-beam three-axis optically pumped magnetometers with sub-100 femtotesla sensitivity,” *Applied Physics Express* **14**, 066002 (5 2021).
- [30] Bamford, R. A., Kellett, B., Bradford, W. J., Norberg, C., Thornton, A., Gibson, K. J., Crawford, I. A., Silva, L., Gargaté, L., and Bingham, R., “Minimagnetospheres above the Lunar Surface and the Formation of Lunar Swirls,” *Physical Review Letters* **109**, 081101 (8 2012).
- [31] Lin, R. P., Mitchell, D. L., Curtis, D. W., Anderson, K. A., Carlson, C. W., McFadden, J., Acuña, M. H., Hood, L. L., and Binder, A., “Lunar surface magnetic fields and their interaction with the solar wind: Results from lunar prospector,” *Science* **281**, 1480–1484 (9 1998).
- [32] Zhang, R., Smith, K., and Mhaskar, R., “Highly sensitive miniature scalar optical gradiometer,” *Proceedings of IEEE Sensors* (1 2017).
- [33] Perry, A. R., Bulatowicz, M. D., Bulatowicz, M. D., Larsen, M., Walker, T. G., and Wyllie, R., “All-optical intrinsic atomic gradiometer with sub-20 fT/cm/Hz^{1/2} sensitivity in a 22 μT earth-scale magnetic field,” *Optics Express, Vol. 28, Issue 24, pp. 36696-36705* **28**, 36696–36705 (11 2020).
- [34] Zhang, G., Lin, Q., Su, S., Zheng, W., and Bi, X., “Vector magnetocardiography measurement with a compact elliptically polarized laser-pumped magnetometer,” *Biomedical Optics Express, Vol. 11, Issue 2, pp. 649-659* **11**, 649–659 (2 2020).